

Nanoscale

Accepted Manuscript



This is an *Accepted Manuscript*, which has been through the Royal Society of Chemistry peer review process and has been accepted for publication.

Accepted Manuscripts are published online shortly after acceptance, before technical editing, formatting and proof reading. Using this free service, authors can make their results available to the community, in citable form, before we publish the edited article. We will replace this *Accepted Manuscript* with the edited and formatted *Advance Article* as soon as it is available.

You can find more information about *Accepted Manuscripts* in the [Information for Authors](#).

Please note that technical editing may introduce minor changes to the text and/or graphics, which may alter content. The journal's standard [Terms & Conditions](#) and the [Ethical guidelines](#) still apply. In no event shall the Royal Society of Chemistry be held responsible for any errors or omissions in this *Accepted Manuscript* or any consequences arising from the use of any information it contains.

Synthesis, Optical and Electrochemical Properties of A- π -D- π -A Porphyrin and its Application as Electron Donor in Efficient Solution Processed Bulk Heterojunction Solar Cells

Challuri Vijay Kumar^a, Lydia Cabau^a, E. N. Koukaras^{c,d}, G. D. Sharma^{b*} and Emilio Palomares^{a, e*}

^aInstitute of Chemical Research of Catalonia (ICIQ), Avda. Països Catalans 16, E-43007 Tarragona, Spain

^bR & D Center for Engineering and Science, JEC group of Colleges, Jaipur Engineering College, Kukas, Jaipur 303101, India.

^cInstitute of Chemical Engineering Sciences, Foundation for Research & Technology, Hellas, Stadiou Str. Platani, Patras, 26504, Greece

^dMolecular Engineering Laboratory, Department of Physics, University of Patras, Patras, 26500, GR, Greece

^eCatalan Institution for Research and Advance Studies (ICREA), Avda. Lluís Companys 23, E-08010 Barcelona, Spain

*Corresponding authors: gdsharma273@gmail.com and sharmagd_in@yahoo.com (G.D, sharma) and epalomares@iciq.es (Emilio Palomares)

Abstract

A conjugated acceptor–donor–acceptor (A- π -D- π -A) with Zn-porphyrin core and di-cyanovinyl substituted thiophene (A) connected at meso positions denoted as **VC62** was designed and synthesized. The optical and electrochemical properties of **VC62** were investigated. This new porphyrin exhibits broad and intense absorption in the visible and near infrared regions. Bulk-heterojunction (BHJ) solution processed organic solar cells based on this porphyrin, as electron donor material, and PC71BM ([6,6]-phenyl C₇₁ butyric acid methyl ester), as electron acceptor material, were fabricated using THF and pyridine/THF solvent exhibiting a power conversion efficiency of 3.65% and 5.24%, respectively. The difference in efficiencies is due to the enhancement of the short circuit current J_{sc} and FF of the solar cell, which is ascribed to a stronger and broader incident photon to current efficiency (IPCE) response and a better balanced charge transport in the device processed with pyridine/THF solvent.

Key words: porphyrin, bulk heterojunction solar cells, power conversion efficiency, solvent additive

Introduction

In recent years, organic solar cells based on bulk heterojunction (BHJ) active layers have attracted much attention because of their advantages for the solution processability of the active layer, potential low cost, light weight, flexibility and their applications for large area devices [1]. Organic BHJ solar cells based on conjugated polymers as electron donor materials and fullerene derivatives as electron acceptor materials, made a great progress in achieving high power conversion efficiency (PCE), by optimizing the structure of conjugated polymers and device architecture. Recently, the encouraging PCE close to 10% has been reported for organic solar cell based on polymer donors and acceptors [2]. In spite of this high performance of the solar cells based on polymers, there are disadvantages for polymer donors, for example, the high molecular weight dispersity and the batch-to-batch reproducibility [3]. Comparing with polymers, small molecules possess the advantages of well-defined molecular structure, definite molecular weight, easier purification and good reproducibility [4]. In recent years, various types of small molecule donors have been designed and employed as donor for the fabrication BHJ organic solar cells [5]. To date, the highest PCEs of solution processed OSCs based on small molecule donors and fullerene acceptors are over 9% [6]. However, the PCE has to be further improved for the commercialization of organic solar cells based on small molecules. Remarkably, there has been a recent report of a small molecule based organic solar cell with a record breaking 12% cell efficiency [7], rendering the small molecule based BHJ organic solar cell devices strong competitors to their counterparts based on polymer donors.

Photosynthetic pigments related to the chlorophylls, such as porphyrins, are particularly good candidates for optical and optoelectronic applications, due to their large molar absorption coefficients, tunable electro-chemical and photophysical properties via central metal insertion and/or introduction of various substituents at the macrocycle peripheral positions [8]. The unique properties of porphyrins, including strong Soret and moderate Q bands [9], fast electron injection, and good photophysical and thermal stability, make them ideal candidates for photovoltaic applications [10]. Despite of successful utilization of porphyrins as sensitizers for dye sensitized solar cells [11] (some of them have displayed a record PCE of 12.3 % [12] and 13 % [11]) and in vacuum processed organic solar cells [13, 14], the use of the porphyrins as donors in solution processed BHJ solar cells is very limited due to the difficulty of their solubility in most of

the common organic solvents. One of the most important requirements of materials used in BHJ active layer for solution processed organic solar cell is their high solubility in common organic solvents. However, the appropriate selection of peripheral substituents can increase the solubility of porphyrins. Matsuo et al have reported the synthesis of soluble porphyrins bearing tetraethyl porphyrin cores [15] with two aromatic and two aliphatic groups in trans positions and used them as donor along with PC60BM as electron acceptor for solution processed BHJ organic solar cells and achieved a PCE of 2.5 % with a high open circuit voltage of 0.92 V. Huang et al. have used a conjugated D-A porphyrin containing benzothiadiazole end capped with 3-hexylthienyl linked by ethylene bridge to a porphyrin core, as donor along with PC₇₁BM as acceptor for BHJ solar cells and reported a PCE of 4.02 % [16]. Peng and co-workers, by employing a porphyrin with two diketopyrrolopyrrole units and ethynyl bridges at meso positions, along with PC60BM as electron acceptor, reported a BHJ organic solar cell with a PCE value of 3.71%, which was significantly improved to 4.78% when the BHJ active layer was processed with pyridine [17]. Sharma et al have recently employed a porphyrin derivative with an ethynylpyridyl group at a meso position, as donor along with PC₇₀BM acceptor for solution processed BHJ organic solar cells and achieved a PCE of 2.54 % [18]. Recently, Peng et al employed a porphyrin molecule with less bulky substituents at periphery as donor material along with PC₆₁BM as acceptor for solution processed organic solar cell and achieved a PCE up to 7.23 % [19].

The thiophene group has been used in metal free organic solar cells [20] to enhance the absorption coefficient of the dye and red-shift its absorption spectrum. This concept has been adopted for porphyrin based DSSC. Thiophene units were used in both β - linked [21] and meso linked [22] porphyrin sensitizers to give efficiencies 4.0 % and 5.1 %, respectively. Cyano (CN)- group is a strong electron withdrawing unit that has been widely adopted in small molecules [23]. Introduction of the CN group in the small molecule change their physical, electrochemical and optical properties and photovoltaic performance. Using a strong π -electron withdrawing moiety provides the possibility to control the absorption spectrum into near infrared region via conjugation with electron rich aromatic units, and its rigid and planar aromatic structure helps to enhance the inter-chain packing of a resulting molecule and therefore leads to very high charge carrier mobility.

Chen et al have used an A-D-A small molecule, which consists of conjugated donor back bone main chain and acceptor terminal units as donor for BHJ solution processed solar cell, and achieved PCE over 8% [24]. An acceptor-donor-acceptor (A- π -D- π -A) molecular structure with a conjugated donor backbone and electron-withdrawing terminal has several advantages for use in BHJ devices: (1) high mobility with planar structure and efficient π - π interactions (2) low band gap resulting from the intramolecular charge transfer and (3) good film quality owing to a long conjugated backbone with dispersed alkyl chains similar to polymers. In this context, we report the design and synthesis of an A- π -D- π -A porphyrin small molecule in which di-cyanovinyl substituted thiophene (A) was linked by ethynylene to the porphyrin core with high solubility. Dicyanovinyl is a strong electron withdrawing unit used in many small molecule organic semiconductors. The ethynylene link makes the dicyanovinyl substituted thiophene moiety coplanar to the porphyrin core thus promoting an extensive π -conjugated region. We have used this porphyrin small molecule as a donor along with the PC₇₁BM as acceptor for the fabrication of BHJ solution processed organic solar cells. Moreover, we have shown that nanomorphology of the VC62:PC₇₁BM active layer could be improved by solvent additive pyridine with enhanced balanced charge transport and the PCE has been achieved up to 5.34 % for optimized BHJ organic solar cell.

Experimental details

Characterization Techniques

UV-vis absorption spectra were measured in a 1 cm path-length quartz cell using a Shimadzu model 1700 spectrophotometer. ¹H NMR spectra were recorded at 300 MHz on a Bruker 300Avance NMR spectrometer with X-WIN NMR software. ¹H spectra were referenced to tetramethylsilane. ESI mass spectra were recorded on a Water Quattro micro (Water Inc, USA). Cyclic voltammetric experiments were carried out with a PC-controlled CH instruments model CHI620C electrochemical analyzer.

Materials

Dichloromethane, Pyrrole, Pyridine, Dichloroethane, Ethanol and THF were distilled before use. The 3, 5 tert butyl benzaldehyde, β -alanine, Malononitrile DDQ, ⁴, Pd₂(dba)₃, AsPh₃, N-bromosuccinimide (NBS), NEt₃, were purchased from Sigma-Aldrich. These precursors are used to synthesize compound 4 as in reference 25.

Synthesis of porphyrin VC62

Synthesis of 3:

A solution consisting of **1** (200 mg, 1.05 mmol) malononitrile (**2**) (209 mg, 3.17mmol) and β -alanine (0.93 mg, 0.010mmol) in a mixture of dichloroethane (6mL) and ethanol (6mL) was stirred under reflux overnight. The mixture was cooled at room temperature and the solvent was removed. The reaction mixture was allowed to cool to room temperature and the precipitate was filtered off and washed thoroughly with ethanol to provide the compound. The crude product was recrystallized from ethanol and the residue of the filtrate purified on a silica column with dichloromethane-petrol ether (1:1). Compound **3** was obtained in a yield of 74%. ^1H NMR (300 MHz, Chloroform-*d*) δ_{H} : 7.74 (s, 1H), 7.50 (d, $J = 4.1$ Hz, 1H), 7.24 (d, $J = 4.1$ Hz, 1H). ^{13}C NMR (126 MHz, CDCl_3) δ 140.60, 129.38, 127.32, 122.56, 117.09, 104.10, 103.27, 69.06

Synthesis of VC62:

In a dry Schlenck tube **4** [25] (50 mg, 0.062 mmol) **3** (37.5 mg, 3.17mmol) were dissolved in a mixture of dry THF (18 mL) and NEt_3 (3.5 mL) and the solution was degassed with di nitrogen for 10 min; $\text{Pd}_2(\text{dba})_3$ (34 mg, 0.03 m mol) and AsPh_3 (76 mg, 0.25 m mol) were added to the mixture. The solution was refluxed for 12 h under nitrogen atmosphere. The solvent was removed under reduced pressure and the crude product was purified by silica gel column chromatography (Dichloromethane:Methanol 6:4) to afford pure product as a green solid (22 mg, yield 32%). ^1H NMR (300 MHz, THF-*d*₈) δ_{H} 9.85 (d, $J = 4.6$ Hz, 4H), 9.14 (d, $J = 4.6$ Hz, 4H), 8.12(S,2H), 8.31 (d, $J = 1.7$ Hz, 4H), 8.14 (d, $J = 3.4$ Hz, 2H), 8.1 (d, $J = 4.0$ Hz, 2H), 8.05 (d, $J = 4.4$ Hz, 2H), 1.79(S, 36H). MS-ESI (m/z): [M] calculated for $\text{C}_{68}\text{H}_{56}\text{N}_8\text{S}_2\text{Zn}$: 1112.34. MALDI-TOF (m/z): [M] calculated for $\text{C}_{68}\text{H}_{56}\text{N}_8\text{S}_2\text{Zn}$: 1112.3361, found 1112.3256

Device fabrication and characterization

The BHJ organic solar cells were fabricated using the glass /ITO /PEDOT:PSS/ VC62:PC₇₁BM/Al device structure. The ITO coated glass substrates were cleaned ultrasonically subsequently in aqueous detergent, de-ionized water, isopropyl alcohol and acetone and finally dried under ambient conditions. An aqueous solution of PEDOT:PSS (Heraeus, Clevious P VP, Al 4083) was spin cast on the ITO substrates to obtain film having a thickness of about 40 nm. The PEDOT:PSS film was then dried for 10 min at a temperature of 120° C in ambient conditions. Mixtures of VC62 with PC₇₁BM with weight ratios of 1:0.5, 1:1, and 1:2 and 1:2.5 in THF were prepared and then spin-cast onto the PEDOT:PSS layer and dried overnight at ambient atmosphere. The devices were further fabricated by the use of 1 %, 2 %, 3 % and 4% pyridine processing additive during

the spin casting step. Finally, the aluminum (Al) top electrode was thermally deposited on the active layer at a vacuum of 10^{-5} Torr through a shadow mask of area of 0.20 cm^2 . All devices were fabricated and tested in ambient atmosphere without encapsulation. The hole-only and electron-only devices with ITO/PEODT:PSS/VC62:PC₇₁BM/Au and ITO/Al/VC62:PC₇₁BM/Al architectures were also fabricated in an analogous way, in order to measure the hole and electron mobility, respectively.

The current-voltage characteristics of the BHJ organic solar cells were measured using a computer controlled Keithley 238 source meter under simulated AM1.5G illumination of 100 mW/cm^2 . A xenon light source coupled with optical filter was used to give the stimulated irradiance at the surface of the devices. The incident photon to current efficiency (IPCE) of the devices was measured illuminating the device through the light source and monochromator and the resulting current was measured using a Keithley electrometer under short circuit condition.

Results and discussion

Synthesis of VC62

The target A- π -D- π -A porphyrin small molecule VC62 was achieved by a convergent synthesis strategy on the basis of sonagashira coupling reaction 2-((5-bromothiophen-2-yl)methylene)malononitrile(3) with di acetylene porphyrin [25] in the presence of dry THF,NEt₃,Pd₂(dba)₃ and AsPh₃. Knoevenagel condensation of malonodinitrile with bromothiophenylaldehyde gave the intrermediate (3). The synthetic route of VC62 is shown in scheme 1. The important intermediates and the targeted small molecule VC62 was well characterized by ¹H-NMR, ¹³CNMR, and ESI mass spectroscopy. In this manuscript a new class of porphyrin small molecule is presented in which the porphyrin central unit contains electron withdrawing di cyano as the end capped group. Introduction of the strongly electron donating group tert butyl of phenyl rings, attached at the meso-positions of the porphyrin core increases the electronic density on the porphyrin π -system and also improves solubility. The general architecture of A- π -D- π -A small molecule and molecular structure of VC62 is shown in scheme 2.

Photophysical and electrochemical properties

Figure 1 shows the absorption spectra of VC62 in dilute THF solution and the thin film cast from the THF solvent. The VC62 exhibits strong Soret band in the range 400 - 540 nm with peak at 482 nm and a moderate Q band in the range 650-760 nm with peak around 710 nm which is typical for ethynyl porphyrins [26]. Compared to other porphyrin

compounds, the Soret band of **VC62** is red shifted and also broadened, and the Q band is also redshifted and intensified, probably due to the intermolecular charge transfer (ICT) between the donor and acceptor units. These spectral changes indicate effective π -elongation through the porphyrin core, ethynyl and di-cyanovinyl substituted thiophene and better conjugation for **VC62** [27]. The absorption spectrum of **VC62** in thin film showed a red shift of 15 nm at Q band region, which, is attributed to the strong intermolecular interaction in solid state. The optical bandgap of the **VC62** is estimated from the onset of the absorption spectrum in thin film and is about 1.58 eV. This porphyrin molecule exhibits high mobilities and wide absorption from 400 to 800 nm with high absorption coefficients owing to the efficient conjugation in the backbone structure and intramolecular charge transfer (ICT) between the terminal acceptor units and the central donor building blocks.

The HOMO and LUMO energy levels were determined by cyclic voltammetry method with a film on platinum wire as working electrode in 0.1M tetrabutylammonium hexafluorophosphate in THF at a potential scan rate of 10 mV s⁻¹, and the counter electrode a platinum mesh. The reference electrode was the silver calomel electrode (saturated KCl). The onset oxidation (E_{onset}^{ox}) and reduction (E_{onset}^{red}) potentials of **VC62** were 1.04 V and -0.74 V vs saturated calomel electrode, respectively, from which the HOMO and LUMO energy levels were estimated using empirical expressions of $E_{HOMO} = -q(E_{onset}^{ox} + 4.40)eV$ and $E_{LUMO} = -q(E_{onset}^{red} + 4.40)eV$, respectively. The estimated values of HOMO and LUMO levels of **VC62** are -5.44 eV and -3.66 eV, respectively. The HOMO-LUMO gap estimated from the cyclic voltammetry is higher than the optical bandgap, which is a common feature in the organic semiconductors. The LUMO gap and HOMO gap between the **VC62** porphyrin (donor) and PCBM (acceptor) are 0.64 eV and 0.36 eV, respectively are large enough to guarantee efficient exciton dissociation at donor/acceptor interfaces exist in the BHJ active layer [28]. The deeper value of HOMO level of **VC62** is beneficial to achieve the high open circuit voltage.

Theoretical calculation

We have performed the theoretical study of **VC62** porphyrin within the framework of density functional theory (DFT) and time dependent density functional theory (TD-DFT). The initial geometry optimization calculations were performed employing the gradient corrected functional PBE [29] of Perdew, Burke and Ernzerhof. The triple- ζ quality TZVP basis set was used for all of the calculations [30]. At this stage of the

calculations, to increase the computational efficiency (without loss in accuracy), the resolution of the identity method was used for the treatment of the two-electron integrals [31]. The resulting structures were further optimized using the hybrid exchange–correlation functional B3LYP [32] and the same basis set. Truhlar’s meta-hybrid exchange–correlation functional M06 [33] was also used for both ground state and excited state calculations. Tight convergence criteria were placed for the SCF energy (up to 10^{-7} Eh) and the one-electron density (rms of the density matrix up to 10^{-8}) as well as for the norm of the Cartesian gradient (residual forces both average and maximum smaller than 1.5×10^{-5} a.u.) and residual displacements (both average and maximum smaller than 6×10^{-5} a.u.). Solvent effects were included for tetrahydrofuran using the integral equation formalism variant of the Polarizable Continuum Model (IEFPCM), as implemented in the Gaussian package [34]. TD-DFT excited state calculations have been performed to calculate the optical gap of the **VC62** porphyrin using the same functionals and basis set on the corresponding ground state structures. The UV/Vis spectra were calculated using the B3LYP and M06 functionals. The first round of geometry optimization was performed using the Turbomole package [35]. All of the follow up calculations were performed using the Gaussian package. [34]

For the geometry optimization of the porphyrin structure a few rotamers were examined as initial geometries. The final optimized structure is a true local (if not global) minimum, as determined by vibrational analysis, i.e. none of the vibrational modes had imaginary eigen frequencies. The main porphyrin part of the **VC62** structure is co-planar with the thiophene and cyano groups. At the optimized geometry the benzene planes form dihedral angles with the plane of the main structure of 71.1° when solvent effects are accounted for THF, and 75.0° in gas phase. We have calculated the HOMO and LUMO energy levels and the optical gaps, defined here as the energetically lowest allowed vertical electronic excitation, employing the PBE, M06, and B3LYP functionals. In Table 1, in addition to the frontier orbitals’ energy levels, we also provide the optical gap the main contributions to the first excitation as well as the wavelength of the first excitation and of the excitations with the largest oscillator strengths. In addition to the B3LYP functional we have also performed our calculations employing the M06 functional. The M06 meta-hybrid functional was chosen since it provides leveled performance over transition types [36, 37]. We provide results using all three functionals, which can additionally be used for comparison with the literature.

The PBE functional underestimates both the HOMO–LUMO (HL) and the optical gaps, as expected. The optical gaps calculated using the hybrid B3LYP and meta-hybrid M06 functionals are practically the same with the later in better agreement to experiment. In Table 1, we also provide the character of the first allowed excitations only for contributions larger than 4%. The first excitation, as calculated by each of the functionals, clearly exhibits a single-configuration character, with only marginal (if any) secondary contributions.

In Figure 2, we have plotted the isosurfaces (isovalue=0.02) of the HOMO and LUMO, as well as the next nearest frontier orbitals, for the porphyrin structure. Both the HOMO and LUMO extend over the main porphyrin structure and the cyano-thiophene moieties, with a varying level of delocalization. The HOMO–1 and LUMO+1 orbitals are localized on different parts of the porphyrin structure, specifically the former over the central porphyrin structure and the latter over the cyano-thiophene groups. To quantify the contributions of the moieties to the frontier orbitals we have calculated the total and partial density of states (PDOS). The PDOS for the porphyrin is shown in Figure 3. We partition **VC62** into the main porphyrin structure, the cyano-thiophene (CNTP), and the di-tert-butylbenzene (1,1-dimethylethylbenzene, BtMe) groups. The contribution of the CNTP and the main porphyrin structure to the HOMO is 35.9% and 61.0% respectively, with only a 3.1% contribution from BtMe. The corresponding contributions to the LUMO are 53.4%, 45.7% and 0.8%, respectively. The first significant contributions (96.0%) from BtMe are noted at lower energies, around -7.2 eV, which corresponds to the HOMO–3 level. Accordingly, significant (above 5.2%) contributions of BtMe to unoccupied states are noted energetically much higher than LUMO, at -0.56 eV, which corresponds to the LUMO+9 level and to which it contributes 96.6%.

In Figure 4a we show the UV/Visual absorption spectra of the **VC62** porphyrin calculated at the TD-DFT/M06 level of theory, both accounting for solvent effects for THF and in gas phase. The spectra have been produced by convoluting Gaussian functions with HWHM = 0.18 eV centered at the excitation wave numbers. In Figure 4b we also provide the corresponding spectra calculated using the B3LYP functional, which is in very good agreement with both that using M06 and the experimental spectra. The Soret band (B band) and Q bands, are noticeable, as expected for porphyrin structures. The wavelengths of the excitations with the largest oscillator strengths for bands are given in Table 1. Compared to the corresponding experimental spectrum

the wave numbers are slightly larger, by about 10–20 nm for the Soret band and by about 35 nm for the Q band. The high intensity Soret band peaks are centered at 496 nm (2.50 eV), 484 nm (2.56 eV) and 439 nm (2.83 eV), that correspond to the 2nd, 3rd and 4th excited states (with non-negligible oscillator strengths). The B band peak is centered at 750 nm (1.65 eV).

Photovoltaic properties

In the organic BHJ solar cells using donor and acceptor materials, relative concentrations of these materials used in the active thin film significantly influences the photovoltaic performance, since there should be a balance between the absorbance and charge transporting network in the active layer. When the concentration of acceptor material is too low, the electron transporting ability will be limited and the higher amount of acceptor concentration, the absorbance and hole transport ability in the active layer will be decreased. BHJ active layers with mixtures of **VC62** and PC₇₁BM blended in THF in different weight ratios were tested, i.e. 1:0.5, 1:1 and 1:1.5. The optimum device performance was found for the 1:1 ratio.

The current voltage (J-V) characteristics under AM1.5 (100 mW/cm²) simulated solar illumination of the BHJ solar cell with the optimized **VC62**:PC₇₁BM (1:1) processed from THF is shown in Figure 5a and the photovoltaic parameters are summarized in table 2. The device showed over all PCE of 3.65 % with J_{sc} = 8.82 mA/cm², V_{oc} = 0.94 V and FF = 0.44. The open circuit voltage of BHJ solar cells using **VC62**:PC₇₁BM processed from THF is about 0.94 V, which is quite high, which may be due to deeper HOMO level of **VC62**, since the V_{oc} of the BHJ organic solar cells is directly related to the energy difference between the HOMO energy level of donor and LUMO energy level of acceptor.

The IPCE values of the solar cell were estimated from the following expression:

$$IPCE(\lambda) = 1240 J_{sc} / \lambda P_{in}$$

Where J_{sc} is the photocurrent under short circuit condition, λ is the wavelength of the incident monochromatic light, and P_{in} is the incident photon flux. The IPCE spectrum of the BHJ solar cell is shown in Figure 5b and found that this spectrum is closely resembles with the optical absorption spectrum of the **VC62**:PC₇₁BM thin film (as shown in Figure 1), indicating that the both **VC62** and PC₇₁BM contributes to the exciton generation after the absorption of photons by the blend thin film. The IPCE values in both

Soret band and Q bands are similar which means that despite the different absorption both electronic transitions are capable to transform with the same efficiency photons to electrons.

The overall PCE of the organic solar cell **VC62**:PC₇₁BM processed with THF solvent is smaller as compared to the latest development in the polymers and small molecules as donor with almost same configuration. Although, the V_{oc} of the present device is quite high ($V_{oc}=0.94$ V), its poor performance can be attributed to the low values of J_{sc} and FF. These two parameters are directly related to the light harvesting efficiency of the BHJ active layer, film morphology, charge transport and their collection on the respective electrodes. In most of the organic BHJ solar cells, the J_{sc} value is related to both electron and hole transport efficiencies within the active layer. The electron mobility is usually much higher than that of hole mobility, resulting in unbalanced charge transport [38]. Moreover, the well defined nanomorphology of the BHJ active layer within the range of exciton diffusion length is necessary for the efficient exciton dissociation [39].

It was reported that the morphology of the BHJ active layers using either polymers or small molecules can be improved by appropriate treatment methodologies which include thermal annealing [40] and solvent additives [41]. Recently, the solvent additive has been also adopted for BHJ thin film using porphyrins as donor and fullerene derivatives as acceptor and the PCE has been significantly improved [19]. We have tried to improve the performance of the BHJ organic solar cells based on **VC62**:PC₇₁BM (1:2) using solvent additive method. We have used pyridine as solvent additive for the deposition of **VC62**:PC₇₁BM active layer. The current–voltage characteristics of the BHJ solar cell processed with 4 % pyridine/THF solvent is shown in Figure 5a and corresponding photovoltaic parameters are displayed in Table 2. We can see that the J_{sc} (10.64 mA/cm²) and FF (0.64) have significantly improved, however, V_{oc} decreased from 0.94 V to 0.88 V, resulting over all PCE of 5.24 %.

The enhancement in the PCE is mainly attributed to the significant increase in values of J_{sc} and FF. The improvement in the value of J_{sc} can be ascribed to the enhancement in the values of IPCE of the device processed with pyridine/THF solvent. As shown in Figure 5b the solar cell with the active layer processed with pyridine/THF exhibits higher values of IPCE and broader IPCE response as compared to the solar cell with the active layer processed with THF only. The J_{sc} value and IPCE response of a solar cell are related by the expression:

$$J_{sc} = \int_{\lambda_1}^{\lambda_2} qIPCE(\lambda)N_{ph}(\lambda)d\lambda$$

where $N_{ph}(\lambda)$ is the photon flux intensity at wavelength λ , q is the electronic charge and λ_1 and λ_2 are the wavelength that correspond to the lower and upper limits of the IPCE spectrum, respectively. The integrated values of J_{sc} from above expression are about 8.56 mA/cm^2 and 10.56 mA/cm^2 for the organic solar cells with active layer processed with THF and pyridine/THF solvents, respectively. These values are consistent with the values observed in J-V characteristics.

In an organic BHJ solar cell, the IPCE is represented by the product of the efficiencies of four sequential steps for charge generation:

$$IPCE = \eta_A \eta_{ED} \eta_{CT} \eta_{CC}$$

Where η_A is the absorption efficiency of the active layer to generate excitons, η_{ED} exciton diffusion efficiency, η_{CT} exciton dissociation to charge transfer, and η_{CC} is the charge collection efficiency at the electrodes. The η_A is related to the absorption profile of the active layer used in the device. The absorption spectra of the VC62:PC₇₁BM blend cast from the pyridine/THF is shown in Figure 6. As shown in this figure, the absorption peak corresponds to the longer wavelength region is red-shifted from 715 nm to 730 nm and also the absorption coefficient is also increased, as compared to that for THF cast blend. Moreover, the blend film also showed a new shoulder peak at 756 nm, which attributed to the formation of vibronic crystalline structure [42] and could be beneficial to the higher hole mobility. This absorption characteristic of the film indicates that the absorption efficiency of the solar cell has been increased and yielded high IPCE values and J_{sc} [43].

The factor that also contributes to the increased PCE of the later device is the change in nanomorphology of the active layer. For the high performance of BHJ organic solar cell, nanoscale phase separation of active layer is one of the morphological requirements i.e. domain size must be in the range of 10-15 nm, which enables a large interfacial area for exciton dissociation. The morphology of the active layer was examined by atomic force microscopy (AFM) technique in tapping mode. The AFM images of BHJ active layer of VC62:PC₇₁BM (1:2) processed with THF and pyridine/THF are shown in Figure 7. The film cast from THF showed smooth surface with root mean square (rms) roughness of 3.45 nm and domain sizes estimated by the cross section profiles are in the

range of 40-50 nm, while the domain sizes reduced to 15-20 nm with surface roughness with 1.45 nm, when the film is cast from pyridine/THF solvent. The reduced domain sizes are beneficial for increasing D-A interfacial area for exciton dissociation to charge transfer efficiency and charge collection efficiency, resulting enhanced values of J_{sc} and PCE [44].

For efficient BHJ organic solar cells, the electron and hole mobilities in the active layer also play an important role, as these should be balanced in order to achieve efficient charge transport. The hole and electron mobilities in the **VC62**:PC₇₁BM blend films were estimated from the hole only device and electron only devices, respectively prepared from THF and pyridine/THF processed films, by means of space charge limited current (SCLC) measurements [45] and the J-V curves are shown in Figure 8a and 8b. The hole mobility and electron mobility are $8.34 \times 10^{-5} \text{ cm}^2/\text{Vs}$ and $2.32 \times 10^{-4} \text{ cm}^2/\text{Vs}$, respectively for devices processed with pyridine/THF, and the ratio of electron to hole mobility is much smaller than the devices fabricated with THF only (hole and electron mobilities are $5.62 \times 10^{-6} \text{ cm}^2/\text{Vs}$ and $2.45 \times 10^{-4} \text{ cm}^2/\text{Vs}$, respectively). Therefore, the addition of pyridine additive improves the hole mobility, but slightly lowers the electron mobility, leading to more balanced charge transport.

Conclusions

In summary, we have synthesized an A-D-A porphyrin **VC62** with a low bandgap (~1.58 eV) and, moreover, we investigated its optical and electrochemical properties (both theoretically and experimentally). The photophysical and electrochemical investigations of **VC62** and PC₇₁BM films probes that the **VC62**:PC₇₁BM blend can effectively harvest photons from visible to near infrared region of solar spectrum and transfer the electrons to PC₇₁BM molecules, resulting in a photovoltaic effect. The solution processed BHJ solar cell based on **VC62**:PC₇₁BM processed from THF solvent displayed a PCE of 3.65 %. In order to improve the PCE of this solar cell, the **VC62**:PC₇₁BM layer was spin cast from a mixture of 4 v% pyridine/THF and the device showed a PCE of 5.24 %, attributed to the enhancement in the J_{sc} and FF. This is a result of the enhanced IPCE response and reduced domain sizes in the active layer, which leads to more balanced charge transport, and enhanced hole mobility in the BHJ active layer.

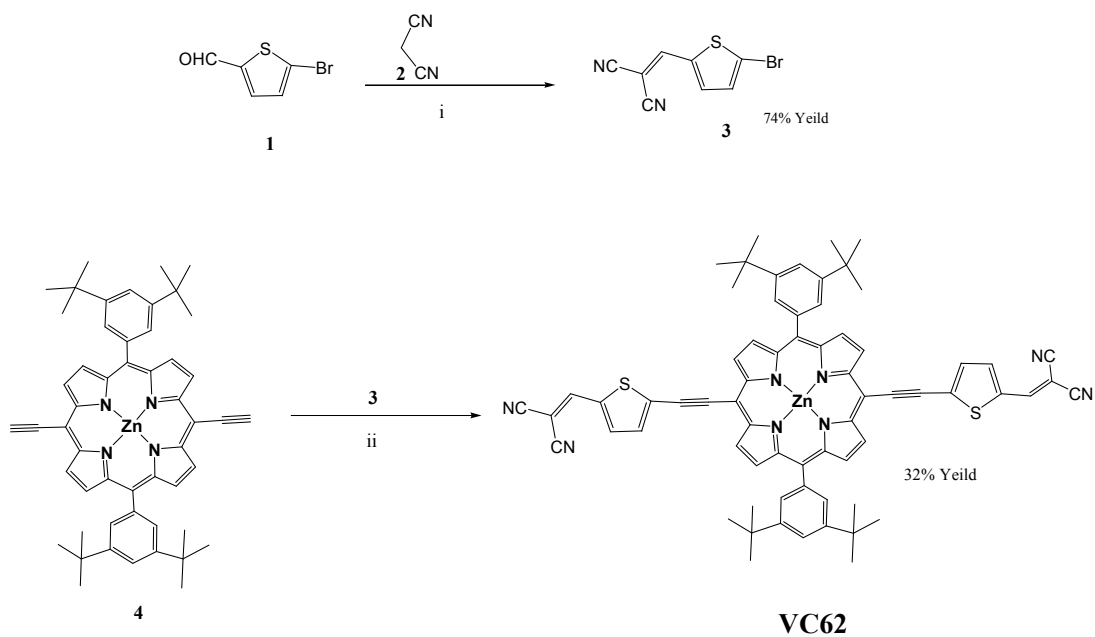
References

1. (a) J. Chen, and Y. Cao, *Acc. Chem. Res.* 2009, **42**, 1709–1718. (b) Y. J. Cheng, s. H. Yang and C.S. Hsu, *Chem. Rev.* 2009, **109**, 5868–5923, (c) G. Li, R. Zhu and Y. Yang, *Nat. Photonics* 2012, **6**, 153–161, (d) Y. Li, *Acc. Chem. Res.* 2012, **45**, 723–733
2. (a) J. You, L. Dou, K. Yoshimura, T. Kato, K. Ohya, T. Moriarty, K. Emery, C.C. Chen, J. Gao, G. Li, and Y. Yang, *Nat. Commun.* 2013, **4**, 1446, (b) Z. C. He, C. M. Zhong, X. Huang, W. Y. Wong, H. B. Wu, L. W. Chen, S. J. Su and Y. Cao, *Adv. Mater.*, 2011, **23**, 4636–4643, (c) Z. C. He, C. M. Zhong, S. J. Su, M. Xu, H. B. Wu and Y. Cao, *Nat. Photonics*, 2012, **6**, 591–595, (d) W. Y. Wong and C. L. Ho, *Acc. Chem. Res.*, 2010, **43**, 1246–1256, (f) M. Wang, X. W. Hu, P. Liu, W. Li, X. Gong, F. Huang and Y. Cao, *J. Am. Chem. Soc.*, 2011, **133**, 9638–9641.
3. A. Salleo, R. J. Kline and D. M. Delongchamp et al. *Adv Mater.*, 2010, **22**, 3812–3838.
4. (a) Y. Lin, Y. Li and X. Zhan, *Chem. Soc. Rev.* 2012, **41**, 4245–4272, (b) Y. Chen, X. Wan and G. Long, *Acc. Chem. Res.*, 2013, **46**, 2645–2655.
5. (a) H. Shang, H. Fan, Y. Liu, W. Hu, Y. Li and X. Zhan, *Adv. Mater.*, 2011, **23**, 1554–1557, (b) Q. Shi, P. Cheng, Y. Li and X. Zhan, *Adv. Energy Mater.*, 2012, **2**, 63–67, (c) T. Bura, N. Leclerc, R. Bechara, P. Lé vê que, T. Heiser and R. Ziessel, *Adv. Energy Mater.*, 2013, **3**, 1118–1124, (d) Y. Liu, Y. M. Yang, C.C. Chen, Q. Chen, L. Dou, Z. Hong, G. Li, and Y. Yang, *Adv. Mater.*, 2013, **25**, 4657–4662, (e) Y. Sun, G.C. Welch, W.L. Leong, C.J. Takacs, G.C. Bazan and A.J. Heeger, *Nat. Mater.*, 2011, **11**, 44–48, (f) T.S. van der Poll, J.A. Love, T.Q. Nguyen and G.C. Bazan, *Adv. Mater.*, 2012, **24**, 3646–3649.
6. (a) V. Gupta, A.K.K. Kyaw, D.H. Wang, S. Chand, G.C. Bazan, A. J. Heeger, *Sci. Rep.* 2013, **3**, 1965, (b) Y. Liu, C. C. Chen, Z. Hong, J. Gao, Y. Yang, H. Zhou, L. Dou, G. Li and Y. Yang, *Sci. Rep.* 2013, **3**, 3356.
7. http://www.heliatek.com/newscenter/latest_news/neuer-weltrekord-fur-organische-solarzellen-heliatek-behauptet-sich-mit-12-zelleffizienz-als-technologiefuhrer/?lang=en Small molecule organic solar cells by Heliatek/IAPP with a certified efficiency of 12.0%”, press release, January 2013; <http://www.heliatek.com> (accessed February 2013).
8. (a) C. W. Lee, H. P. Lu, C. M. Lan, Y. L. Huang, Y. R. Liang, W. N. Yen, Y. C. Liu, Y. S. Lin, E. W. G. Diau and C. Y. Yeh, *Chem.–Eur. J.*, 2009, **15**, 1403; (b) C. L. Mai, W. K. Huang, H. P. Lu, C. W. Lee, C. L. Chiu, Y. R. Liang, E. W. G. Diau and C. Y. Yeh, *Chem. Commun.*, 2010, **46**, 809.

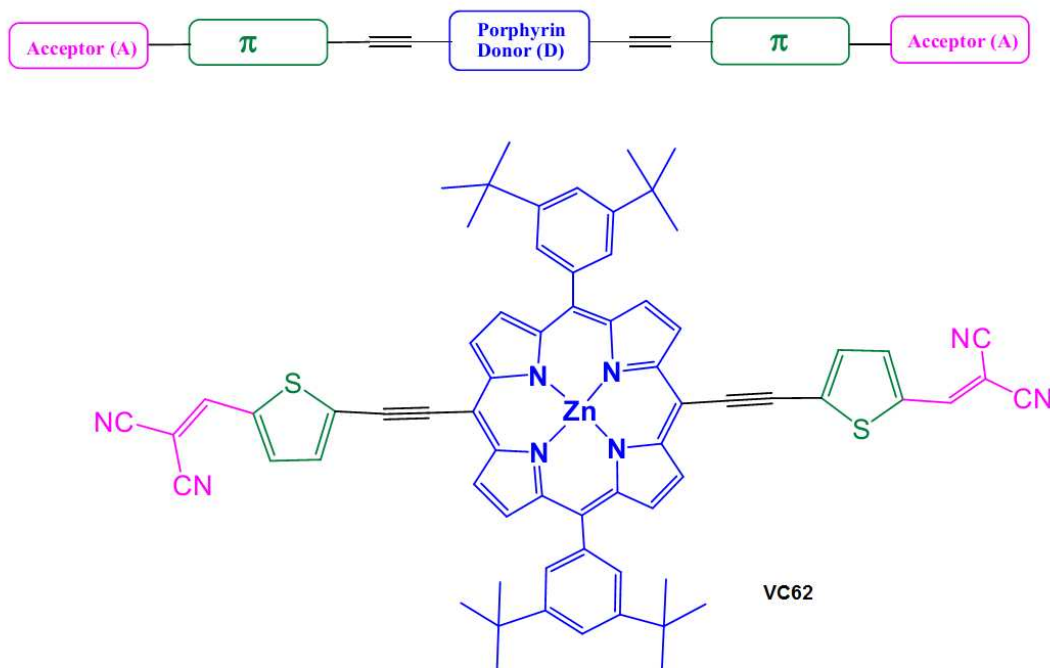
9. (a) A. Kay and M. Grätzel, *J. Phys. Chem.*, 1993, **97**, 6272; (b) M. S. Kang, J. B. Oh, K. D. Seo, H. K. Kim, J. Park, K. Kim and N. G. Park, *J. Porphyrins Phthalocyanines* 2009, **13**, 798.
10. L.-L. Li and E. W.-G. Diau, *Chem. Soc. Rev.*, 2013, **42**, 291–304.
11. (a) N. M. Reddy, T. Y. Pan, Y. C. Rajan, B. C. Guo, C. M. Lan, E. W. G. Diau and C. Y. Yeh, *Phys. Chem. Chem. Phys.*, 2013, **15**, 8409, (b) S. H. Kang, I. T. Choi, M. S. Kang, Y. K. Eom, M. J. Ju, J. Y. Hong, H. S. Kang and H. K. Kim, *J. Mater. Chem. A*, doi: 10.1039/c3ta01128c, (c) S. Mathew, A. Yella, P. Gao, R. Humphry-Baker, Basile F.E. Curchod, N. Ashari-Astani, I. Tavernelli, U. Rothlisberger, M. K. Nazeeruddin and M. Grätzel, *Nature Chem.* 2014, **6**, 242, (d) K. Ladomenou, T. N. Kitsopoulos, G. D. Sharma and A. G. Coutsolelos, *RSC Advances* 2014, **4**, 21379
12. A. Yella, H.W. Lee, H.N. Tsao, C. Yi, A. K. Chandiran, M. K. Nazeeruddin, E. W. G. Diau, C. Y. Yeh, S.M. Zakeeruddin and M. Grätzel, *Science* 2011, **334**, 629–634.
13. (a) Y. Shao and Y. Yang, *Adv. Mater.*, 2005, **17**, 2841; (b) Z.-X. Xu, V. A. L. Roy, Z.-T. Liu and C. S. Lee, *Appl. Phys. Lett.*, 2010, **97**, 163301.
14. (a) Y. Matsuo, Y. Sato, T. Niinomi, I. Soga, H. Tanaka and E. Nakamura, *J. Am. Chem. Soc.*, 2009, **131**, 16048; (b) S. Ito, T. Murashima, H. Uno and N. Ono, *Chem. Commun.*, 1998, 1661; (c) S. Aramaki, Y. Sakai and N. Ono, *Appl. Phys. Lett.*, 2004, **84**, 2085.
15. (a) J. Hatano, N. Obata, S. Yamaguchi, T. Yasuda and Y. Matsuo, *J. Mater. Chem.* 2012, **22**, 19258.
16. Y. Huang, L. Li, X. Peng, J. Peng and Y. Cao, *J. Mater. Chem.* 2012, **22**, 21841.
17. L. Li, Y. Huang, J. Peng, Y. Cao and X. Peng, *J. Mater. Chem. A* 2013, **1**, 2144–2150.
18. G. D. Sharma, D. Daphnomili, S. Biswas and A. G. Coutsolelos, *Org. Electron.* 2013, **14**, 1811
19. H. Qin, L. Li, F. Guo, S. Su, J. Peng, Y. Cao and X. Peng, *Energy Environ. Sci.* doi: 10.1039/c3ee43761b.
20. (a) N. Robertson, *Angew. Chem., Int. Ed.*, 2006, **45**, 2338, (b) Y. Ooyama and Y. Harima, *Eur. J. Org. Chem.*, 2009, 2903–2934, (c) A. Mishra, M. K. R. Fischer and P. Bäuerle, *Angew. Chem. Int. Ed.*, 2009, **48**, 2474–2499, (d) Z. J. Ning, Y. Fu and H. Tian, *Energy Environ. Sci.*, 2010, **3**, 1170.
21. V. A. Nuay, D.-H. Kim, S.-H. Lee and J. J. Ko, *Bull. Korean Chem. Soc.*, 2009, **30**, 2871.

22. Y. Liu, N. Xiang, X. Feng, P. Shen, W. Zhou, C. Weng, B. Zhao and S. Tan, *Chem. Commun.*, 2009, 2499.
23. (a) R. Fitzner, C. Elschner, M. Weil, C. Uhrich, C. Körner, M. Riede, K. Leo, M. Pfeiffer, E. Reinold, E. M.- Osteritz and P. Bäuerle, *Adv. Mater.*, 2012, **24**, 675; (b) A. Gupta, A. Ali, A. Bilic, M. Gao, K. Hegedus, B. Singh, S. E. Watkins, G. J. Wilson, U. Bach and R. A. Evans, *Chem. Commun.*, 2012, **48**,1889;(c) Y. Z. Lin, Z. G. Zhang, H. T. Bai, Y. F. Li and X. W. Zhan, *Chem. Commun.*, 2012, **48**, 9655; (d) S. H. Zeng, L. X. Yin, C. Y. Ji, X. Y. Jiang, K. C. Li, Y. Q. Li and Y. Wang, *Chem. Commun.*, 2012, **48**, 10627; (e) M. Charlotte, S. Gurunathan, A. Magali, K. V'aclav, S. Jiř'ı, F. Pierre and R. Jean, *J. Org. Chem.*, 2012, **77**,2041.(f) N. F. Montcada, B. Pelado, A. Viterisi, J. Albero, J. Coro, P. de la Cruz, F. Langa and E.Palomares *Org. Electron.*, **2013**, **14**, 2826-2832
24. J. Zhou, Y. Zuo, X. Wan, G. Long, Q. Zhang, W. Ni, Y. Liu, Z. Li, G. He, C. Li, B. Kan, Y. Chen, *J. Am. Chem. Soc.*, 2013, **135**, 8484.
25. M. J. Plater, S. Aiken and G. Bourhill, *Tetrahedron* 2002, **58**, 2405
26. T. E. O. Screen, K. B. Lawton, G. S. Wilson, N. Dolney, R. Ispasoiu, T. Goodson III, S. J.Martin, D. D. C. Bradley and H. L. Anderson, *J. Mater. Chem.*, 2001, **11**, 312.
27. (a) H. Imahori, T. Umeyama and S. Ito, *Acc. Chem. Res.*, 2009, **42**, 1809; (b) V. S-Y. Lin, S. G. DiMugno and M. J. Therien, *Science*, 1994, **264**, 1105, (c) C. Y. Lee, C. She, N. C. Jeong and J. T. Hupp, *Chem. Commun.*, 2010, **46**, 6090
28. C. J. Brabec, C. Winder, N. S. Sariciftci, J. C. Hummelen, A. Dhanabalan, P. A. van Hal and R. A. J. Janssen, *Adv. Funct. Mater.*, 2002, **12**, 709
29. J. P. Perdew, K. Burke, M. Ernzerhof, *Phys. Rev. Lett.* 1996, **77**, 3865
30. A. Schäfer, C. Huber, R. J. Ahlrichs, *Chem. Phys.* 1994, **100**, 5829.
31. K. Eichkorn, O. Treutler, H. Öhm, M. Häser, R. Ahlrichs, *Chem. Phys. Lett.* 1995, **240**, 283.
32. (a) A. D. Becke, *J. Chem. Phys.*, 1993, **98**, 5648, (b) C. Lee, W. Yang, R. G. Parr, *Phys. Rev. B* 1988, **37**, 785.
33. Y. Zhao and D. G. Truhlar, *Theor. Chem. Acc.*, 2008 **120**, 215
34. Frisch, M. J.; Trucks, G. W.; Schlegel, H. B.; Scuseria, G. E.; Robb, M. A.; Cheeseman, J. R.; Scalmani, G.; Barone, V.; Mennucci, B.; Petersson, G. A.; Nakatsuji, H.; Caricato, M.; Li, X.; Hratchian, H. P.; Izmaylov, A. F.; Bloino, J.; Zheng, G.; Sonnenberg, J. L.; Hada, M.; Ehara, M.; Toyota, K.; Fukuda, R.; Hasegawa, J.; Ishida, M.; Nakajima, T.; Honda, Y.; Kitao, O.; Nakai, H.; Vreven, T.; Montgomery, Jr., J. A.; Peralta, J. E.; Ogliaro, F.; Bearpark, M.; Heyd, J. J.; Brothers, E.; Kudin, K. N.; Staroverov, V. N.; Kobayashi, R.; Normand, J.; Raghavachari, K.; Rendell, A.; Burant, J. C.; Iyengar, S. S.; Tomasi, J.; Cossi, M.; Rega, N.; Millam, J. M.; Klene, M.; Knox, J. E.; Cross, J. B.; Bakken, V.; Adamo,

- C.; Jaramillo, J.; Gomperts, R.; Stratmann, R. E.; Yazyev, O.; Austin, A. J.; Cammi, R.; Pomelli, C.; Ochterski, J. W.; Martin, R. L.; Morokuma, K.; Zakrzewski, V. G.; Voth, G. A.; Salvador, P.; Dannenberg, J. J.; Dapprich, S.; Daniels, A. D.; Farkas, O.; Foresman, J.B.; Ortiz, J.V.; Cioslowski, J.; Fox, D. J. Gaussian 03, revision C.01; Gaussian, Inc.: Wallingford CT, 2004.
35. TURBOMOLE (version 5.6); Universitat Karlsruhe, 2000.
36. D. Jacquemin, E. A. Per ète, I. Ciofini, Adamo, R. Valero, Y. Zhao and D. G. Truhlar, *J. Chem. Theory Comput.*, 2010, **6**, 2071.
37. S. Mathew, A. Yella, P. Gao, R. Humphry-Baker, F. E. Curchod, N. Ashari-Astani, I. Tavernelli, U. Rothlisberger, M. K. Nazeeruddin and M. Gratzel, *Nature Chem.* 2014, **6**, 242.
38. V. D. Mihailetschi, H. Xie, B. de Boer, L. J. A. Koster and P. W. M. Blom, *Adv. Funct. Mater.*, 2006, **16**, 699.
39. Y. Li, *Acc. Chem. Res.*, 2012, **45**, 723.
40. Y. Zuo, N. Wang, Z. Qian, M. Li, B. Kan, X. Wan and Y. Chen, *J. Mater. Chem. C* doi: 10.1039/c4tc00994k.
41. (a) Y. Chen, X. Wan and G. Long, *Acc. Chem. Res.*, 2013, **46**, 2645, (b) J. E. Coughlin, Z. B. Henson, G. C. Welch and G. C. Bazan, *Acc. Chem. Res.*, 2013, **47**, 257.
42. (a) F.-C. Chen, H.-C. Tseng and C.-J. Ko, *Appl. Phys. Lett.*, 2008, **92**, 103316, (b) J. Hou, H. Y. Chen, S. Zhang, G. Li and Y. Yang, *J. Am. Chem. Soc.*, 2008, **130**, 16144.
43. J. Peet, J. Y. Kim, N. E. Coates, W. L. Ma, D. Moses, A. J. Heeger and G. C. Bazan, *Nat. Mater.*, 2007, **6**, 497
44. (a) W. L. Leong, G. C. Welch, J. Seifert, J. H. Seo, G. C. Bazan and A. J. Heeger, *Adv. Energy Mater.*, 2013, **3**, 356, (b) M.-S. Su, C.-Y. Kuo, M.-C. Yuan, U. S. Jeng, C.-J. Su and K.-H. Wei, *Adv. Mater.*, 2011, **23**, 3315, (c) C. H. Woo, P. M. Beaujuge, T. W. Holcombe, O. P. Lee and J. M. J. Frechet, *J. Am. Chem. Soc.*, 2010, **132**, 15547
45. G. Malliaras, J. Salem, P. Brock and C. Scott, *Phys. Rev. B: Condens. Matter Mater. Phys.*, 1998, **58**, 13411.



Scheme 1: Synthetic route of **VC62**. (Reaction conditions): (i) β -alanine, Dichloroethane, Ethanol, Reflux, Overnight, 74% Yield. (ii) $\text{Pd}_2(\text{dba})_3$, AsPh_3 , dry THF, NEt_3 , reflux 12 h, 32% Yield.



Scheme 2 General architecture of **A- π -D- π -A** small molecule and Molecular structure of **VC62**

Table 1 Calculated properties of **VC62** porphyrin. Specifically HOMO and LUMO energies (eV), HOMO-LUMO gap (eV), HL, optical bandgap (eV) with corresponding oscillator strengths, f , the wavelengths of the first excitation and excitations with the largest oscillator strengths, the main contributions to the first excited state, and the dipole moment (D), μ .

	HOMO (eV)	LUMO (eV)	HL (eV)	OG (eV)	$\lambda_{1st\ max}$ (nm)	f	Main contributions	μ (D)
PBE	-5.24	-4.11	1.13	1.52	814	1.56	H→L (95.7 %)	0.07
B3LYP	-5.68	-3.77	1.91	1.74	712/498/44 7/404/346	1.68	H→L 95.4%; H-1→L+2 (4.6%)	0.07
	-5.51 ^a	-3.67 ^a	1.84 ^a	1.60 ^a	775/504/45 6/415/355 ^a	2.11 ^a	H→L (97.3%) ^a	0.21 ^a
M06	-5.86	-3.64	2.22	1.78	697/485/47 1/430/394/ 333	1.49	H→L (90.1%); H-1→L+2 (7.2%)	0.06
	-5.71 ^a	3.55 ^a	2.15 ^a	1.65 ^a	750/496/48 4/439/405 ^a	1.92 ^a	H→L (93.9%); H-1→L+2 (4.0%) ^a	0.21 ^a

^aValues when solvent effect are taken into account for THF

Table 2 Photovoltaic parameters of the BHJ organic solar cells based on differently processed active layers of **VC62:PC₇₁BM** in 1:1 Weight Ratio

Active layer	J_{sc} (mA/cm ²)	V_{oc} (V)	FF	PCE (%)
VC62:PC₇₁BM (THF cast)	8.82	0.94	0.44	3.65
VC62:PC₇₁BM (pyridine/ THF cast)	10.64	0.88	0.56	5.24

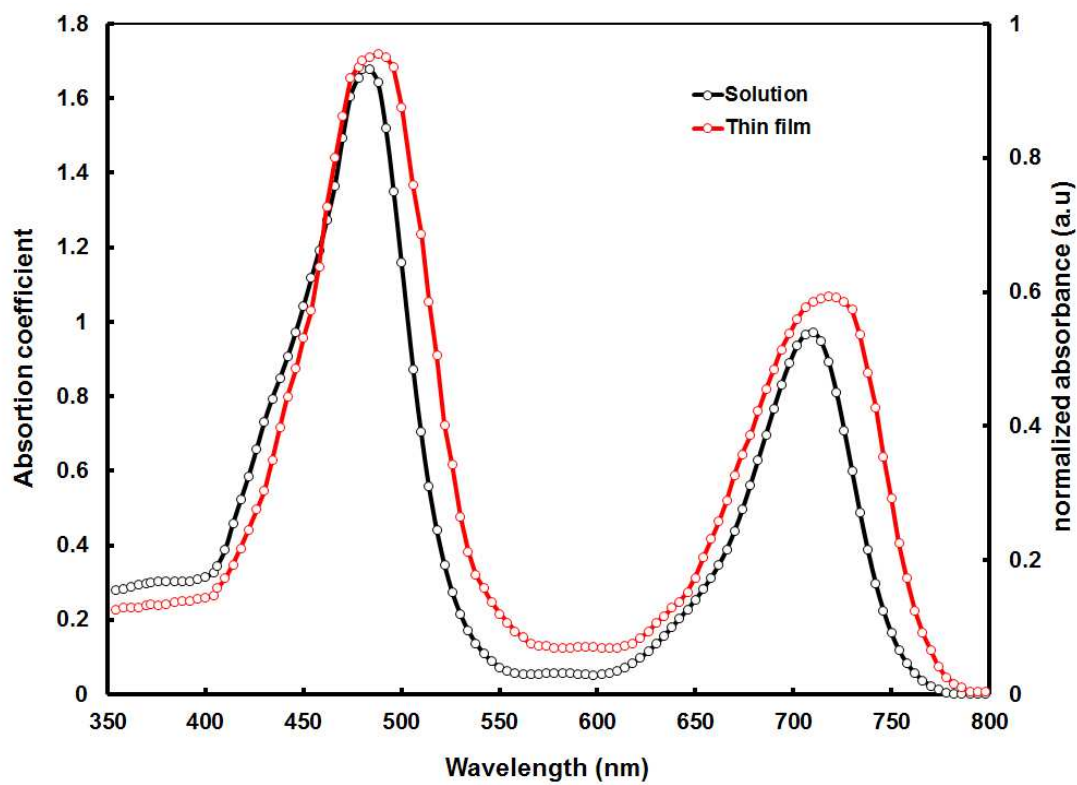


Figure 1 Optical absorption spectra of porphyrin VC62 in THF solution and thin film cast from THF solvent.

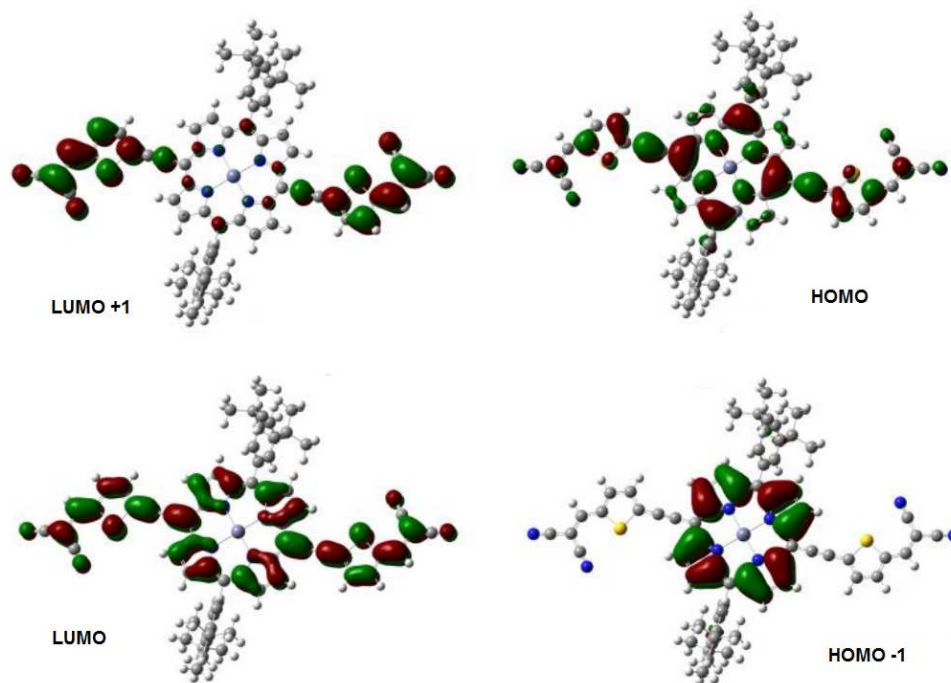


Figure 2 Frontier and near frontier orbital of the VC62 porphyrin

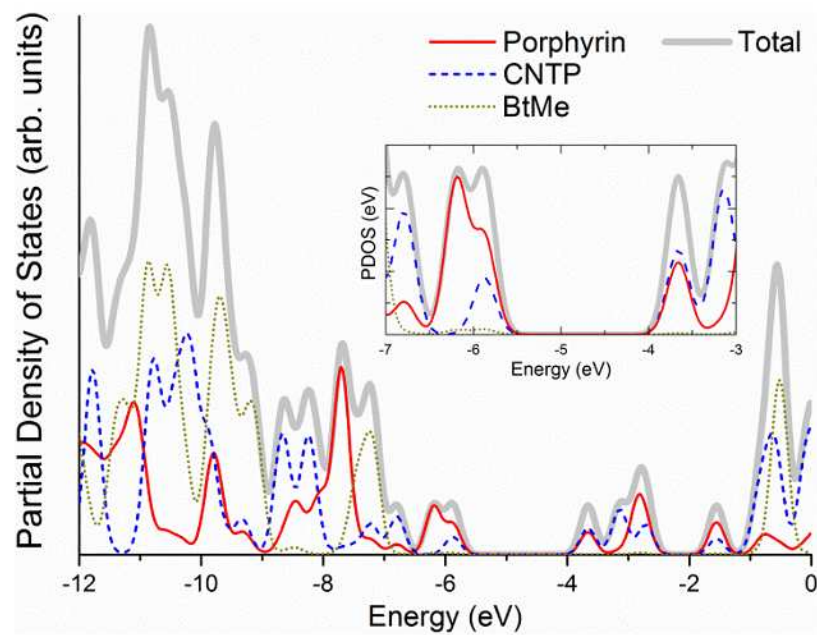


Figure 3 Total and partial density of states of the VC62 porphyrin (calculated using the M06 functional)

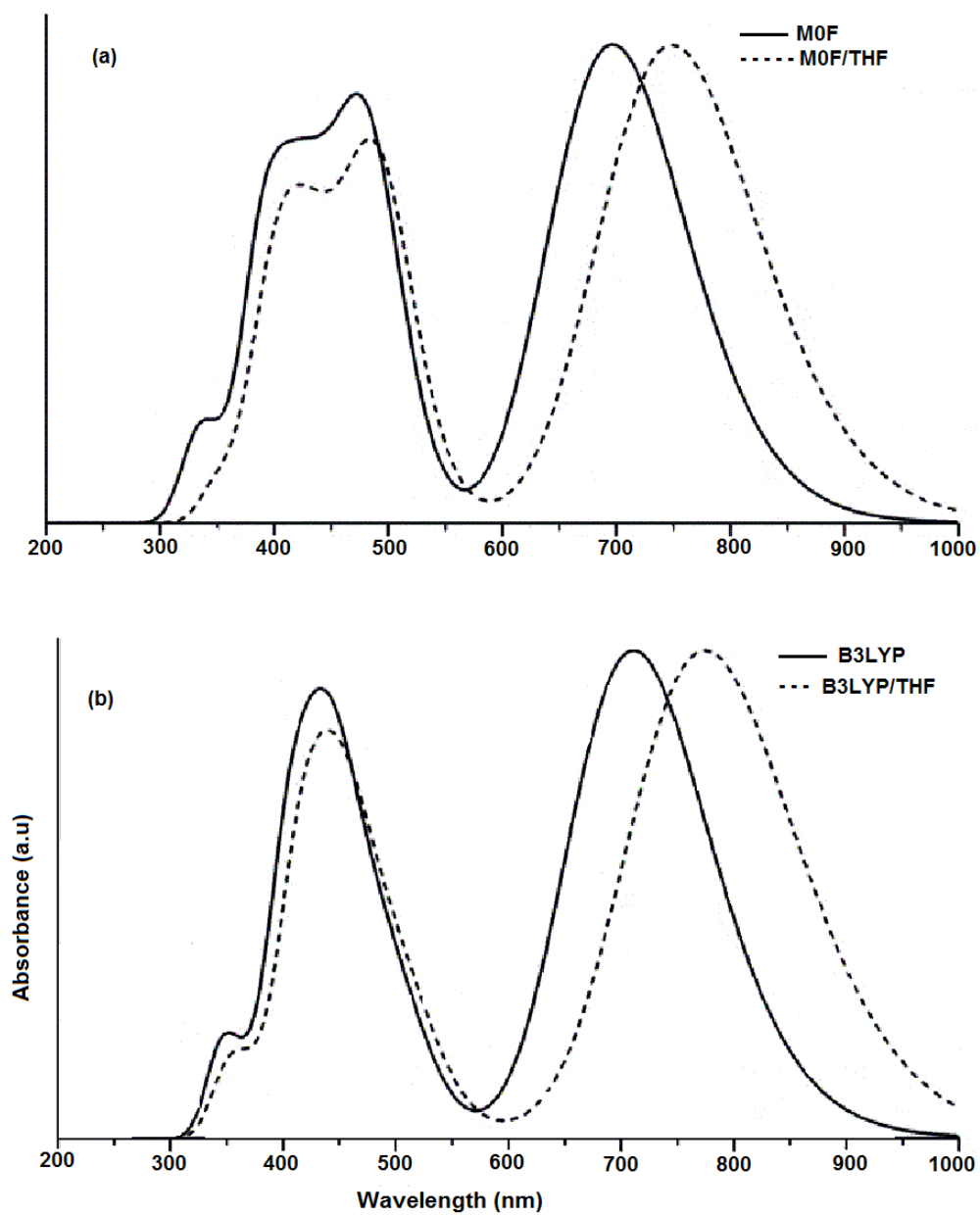


Figure 4 Theoretical absorption spectrum of the VC62 porphyrin calculated using (a) MOF and (b) B3LYP functional

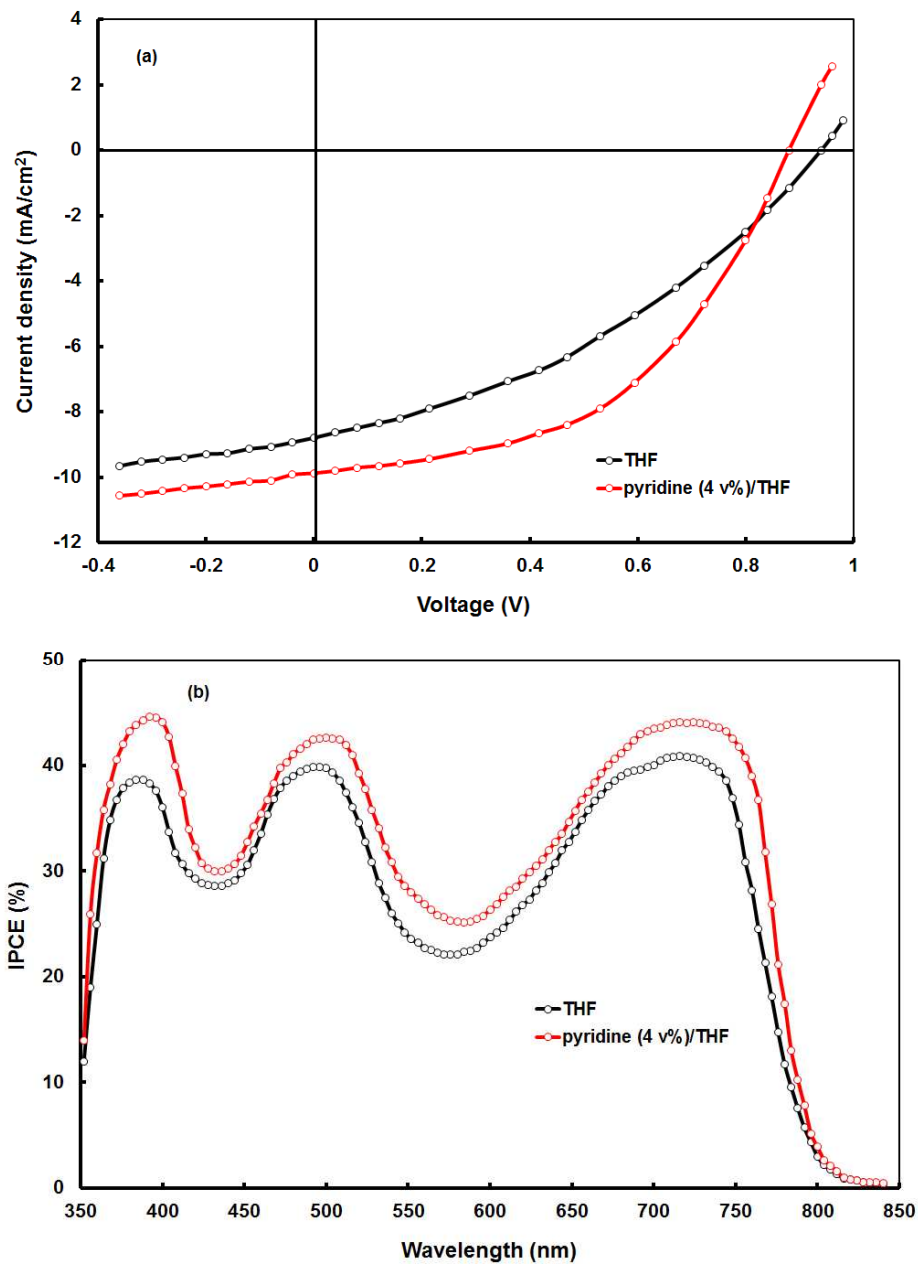


Figure 5 (a) Current-voltage (J–V) characteristics under illumination, and (b) IPCE spectra of the BHJ organic solar cells based on differently processed active layers of VC62:PC₇₁BM

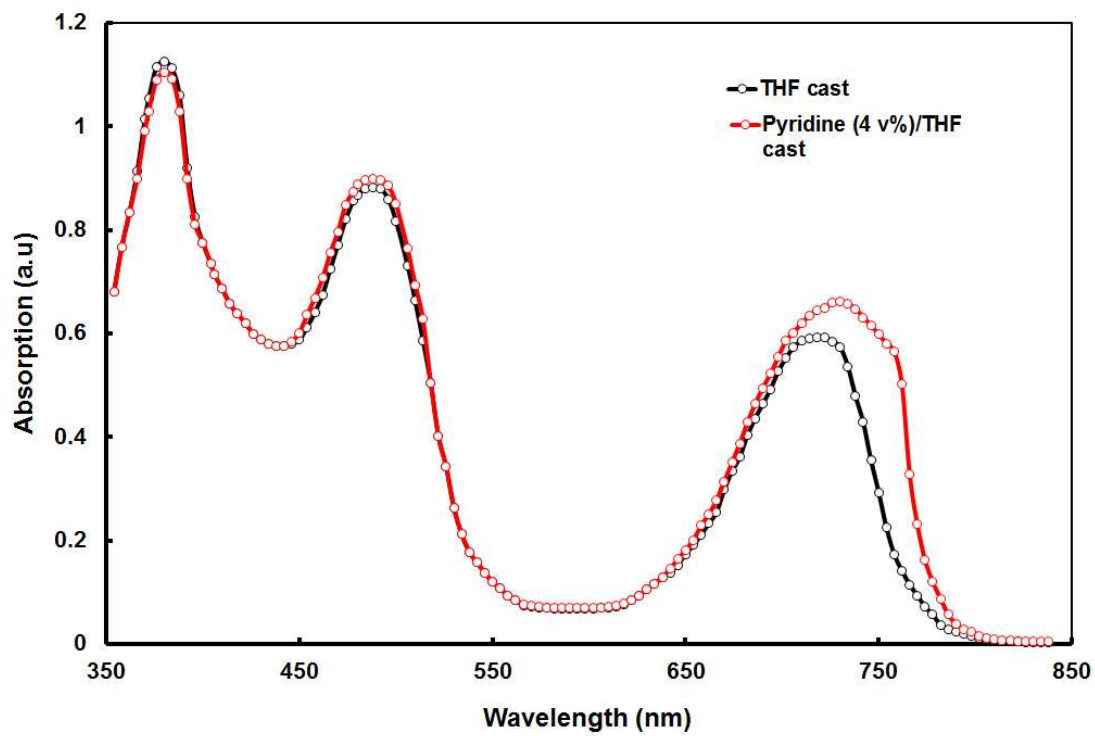


Figure 6 Optical absorption spectra of the VC62:PC₇₁BM thin films cast from THF and pyridine/THF solvents

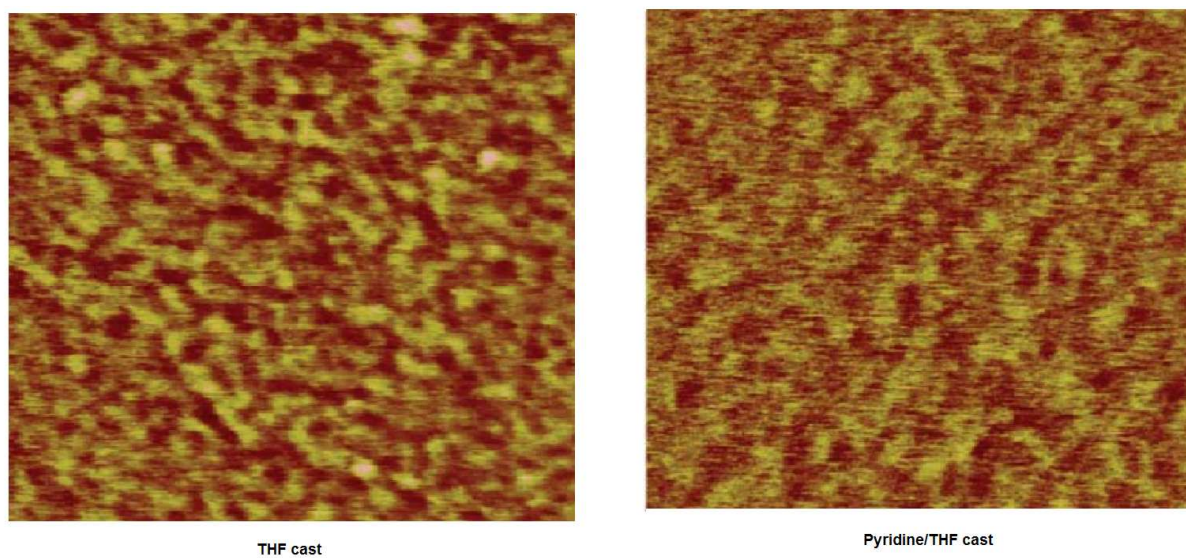


Figure 7 AFM images of VC62:PC₇₁BM thin films cast from THF and pyridine/THF solutions.

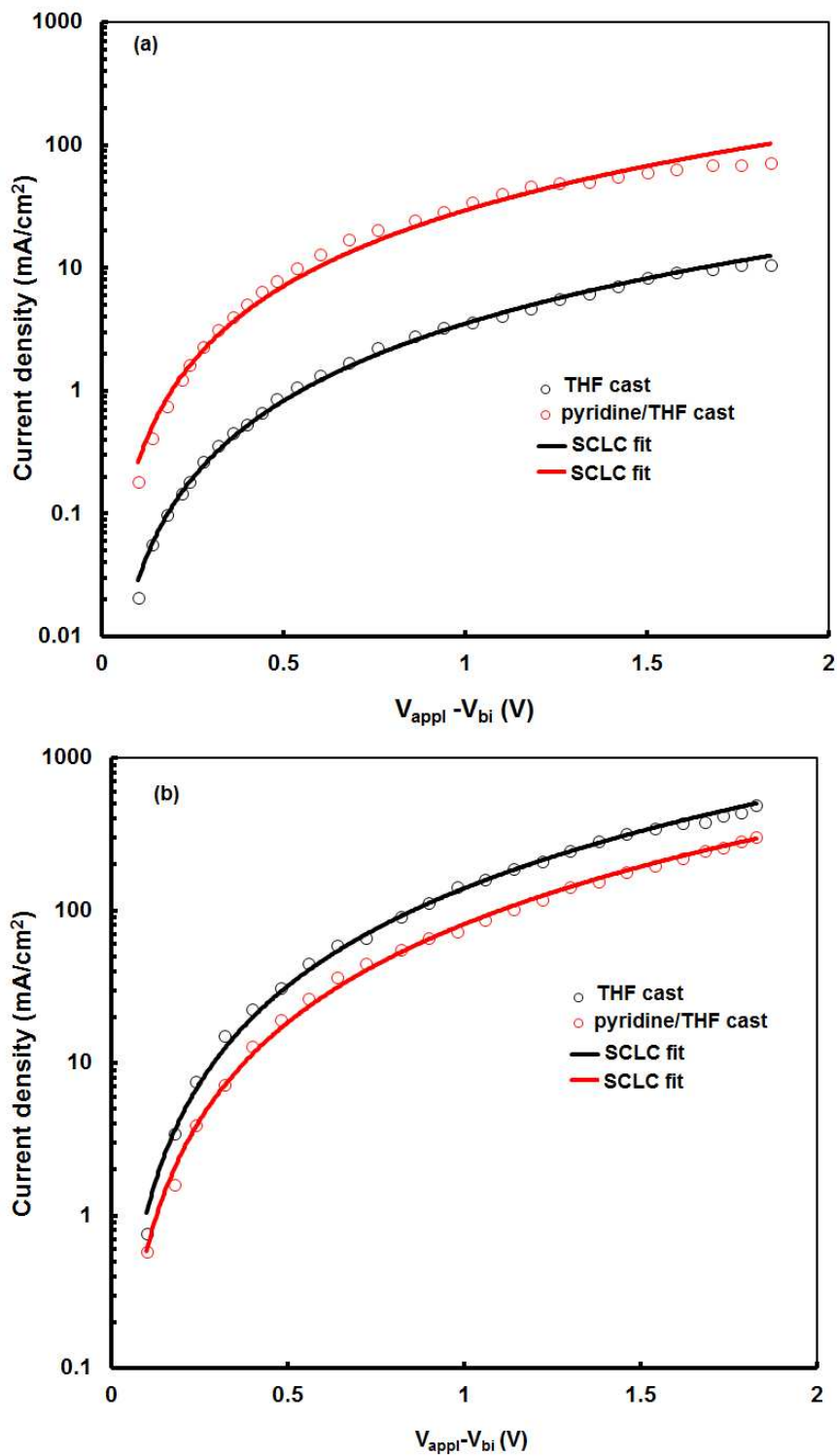


Figure 8 Current-voltage ($J-V$) characteristics in dark for (a) hole-only and (b) electron-only solar cell devices, using two differently processed VC62:PC₇₁BM active layer blends